Author's Accepted Manuscript

Thermophysical and radiative properties of pressureless sintered SiC and ZrB_2-SiC laminates

Elisa Padovano, Claudio Badini, Konstantina Mergia, Jorge Barcena

Thermophysical and radiative properties of pressureless sintered SiC and ZrB$_2$-SiC laminates.

Elisa Padovano[a*], Claudio Badini[a], Konstantina Mergia[b], Jorge Barcena[c]

[a]Politecnico di Torino, Department of Applied Science and Technology, Corso Duca degli Abruzzi, 24, 10129 Torino, Italy
[b]N.C.S.R "Demokritos", Institute of Nuclear and Radiological Science and Technology, Energy and Safety, Aghia Paraskevi, 15310 Athens, Greece
[c]Tecnalia Research & Innovation, Industry and Transport Division, C/Geldo, Edificio 700, E-48160 Derio – Bizkaia, Spain.

[*]Corresponding author. elisa.padovano@polito.it (E. Padovano)

Abstract

The evaluation of thermal and radiative properties of materials to be used as a hot part of thermal protection systems is a key issue for the design process of the HTC and UHTC components. Ceramic laminates with composition 100 vol%SiC and 80 vol%ZrB$_2$-20 vol%SiC were prepared by the tape casting technique and pressureless sintered. Thermal properties such as the thermal expansion coefficient, specific heat, thermal diffusivity and conductivity were measured; in addition the total emissivity was evaluated. A comparison of the thermal behavior of these two kinds of laminates is made. Moreover their possible integration in a unique structure is discussed.

Keywords: Thermal protection system; Silicon carbide; Ultra-high temperature ceramics; Thermal properties; Emissivity

1.   Introduction

The severe environmental conditions a space vehicle is subjected during the Earth re-entry phase involve very high temperatures, significant heating rates, thermal gradients

1

and heat fluxes in addition to high mechanical and thermo-mechanical loads. Thermal Protection Systems (TPS) are indispensable for the protection of the vehicle structure from these severe conditions.

Different TPS technologies have previously been designed: ablative TPS used on the Apollo capsules [1] and interplanetary entry probes [2], or reusable TPS integrating insulated [3] or stand-off structures [4]. Moreover, thanks to the increasing interest in reducing the cost of space access for reusable launch vehicles (RLVs) [5,6] new metallic TPS concepts have also been developed [7,8].

The long service life in harsh environmental conditions makes surface components an essential part of materials technology development for aerospace applications. In fact, due to their specific design, re-entry vehicles usually require control surfaces which include wing leading edges and nose caps. The temperature at the tip of the leading edge is inversely proportional to the square-root of the leading edge nose radius [9], so a small curvature radius results in a very high surface temperature which can exceed 2273K [10].

For the design of this hot part, the attention has focused on Ultra High Temperature Ceramics (UHTCs) due to their high melting point, high hardness and a suitable combination of thermal properties; among them the diborides show some of the highest known melting points (3518 K for ZrB_2, 3653 K for HfB_2 and 3490 K for TiB_2), high thermal and electrical conductivities, high chemical stability and great thermal shock resistance [11].

The main limitation when using these materials for high temperature structural applications is their low intrinsic sinterability which makes it imperative to use very

2

high temperature and high pressure for the sintering ; moreover their oxidation resistance frequently needs to be improved. To overcome this problem different sintering aids can be added to diborides: in the case of ZrB_2-based UHTC the addition of SiC offers many advantages such as an improvement in ZrB_2 sinterability, microstructure refinement promotion and an increase of the oxidation resistance [12–15].

The parts of the vehicle which are further away from the leading edges are subject to a smaller heat flux which is inversely proportional to the square-root of the distance from the stagnation point [9]. For these parts of the vehicle which are only moderately loaded, more conventional materials can be used. For instance SiC is one of the most used materials for high temperature applications due to the formation of a passive silica layer on its surface which prevents a further oxygen penetration up to 1873 K [16]. At higher temperatures the melting of the silica and the mechanism of active oxidation limit the use of this ceramic compound [17,18].

Different materials can be integrated and used for the different parts of the TPS vehicle depending on the environmental conditions they have to face. In this context the European project SMARTEES (Multifunctional component for aggressive environment in space applications) aimed to develop new multifunctional structures to be used as TPS for reusable space vehicles for orbital re-entry [19]. The TPS incorporated components with very different properties: the external part consisted of ceramic laminates based on high temperature ceramics (HTCs) and ultrahigh temperature ceramics while an intermediate SiC foam with skins of conventional CMCs was designed for providing thermal insulation and mechanical strength. A SiC based multilayer system was developed for the back shield part of the re-entry vehicle which

3

is only moderately loaded; ZrB_2/SiC composite multilayers were instead mainly designed for the front shield where the operating conditions are more severe in term of temperature and thermal loads, compared to the back shield.

Most of the literature about re-usable TPSs focuses on the investigation of mechanical properties and oxidation resistance of HTCs and UHTCs. In contrast little data are available about the thermal and radiative properties of these materials, especially at high temperatures.

The performance of the vehicle surface components is strongly dependent on the material interaction with the surrounding environment and consequently on some of its temperature-dependent properties. For this reason the thermal conductivity, the thermal expansion and the thermal shock resistance need to be investigated not only at room temperature but at temperatures as close as possible to those required for aerospace applications. Emissivity is another important factor to be taken into account because of its great influence on the overall heat flow involved during re-entry and consequently on the temperature of the vehicle surface.

The investigation of these properties is also important in order to acquire an accurate materials database for thermal analysis and design.

In the present work the total emissivity, the thermal diffusivity and conductivity, and the coefficient of the thermal expansion of SiC and its composite 80vol%ZrB_2-20vol%SiC, are investigated up to 1800 K. The main goal is to compare the thermal properties of these two materials for applications at high and very high temperatures.

2. Materials and methods

2.1 Laminate fabrication

4

Ceramic laminates were produced according to a process involving several steps: the preparation of a ceramic-based slurry, tape casting of it in order to obtain green tapes, stacking of them in a multilayer structure, de-binding treatment and pressureless sintering.

The slurries were obtained by mixing SiC and/or ZrB_2 powders with sintering aids (boron and carbon were added as sintering additives for SiC in amount of 1 wt% and 3 wt% respectively) in a mixture of solvents. Firstly the powders and the solvents were mixed for 24 hours in an alumina jar containing alumina milling bodies, then the plasticizer and the binder were added and the slurry was further mixed for additional 48 hours. Zirconium diboride powder (Grade B, H.C. Starck, Germany, with an average particle size of 2.25 μm), α-SiC powder (H.C. Starck UF-15, Germany, with a mean particle size of 0.55 μm), carbon in form of graphite (Alfa Aesar flakes 7–10 μm), boron (H.C. Starck amorphous grade I, 1–2 μm), polyethylenglycole (Bisoflex 102 Cognis) and polyvinilbutyral (Butvar B76 Solutia) were used for the preparation of the slurries. More details about the chemical composition of the slurries, specifically the relative amount of the different components, are reported elsewhere [20]. The prepared slurries were cast on a movable Mylar support with an advance speed of 100 mm/min and setting the height of doctor blade at 1 mm. A slow drying of the cast slurry at room temperature allowed to obtain the so called "green" tapes, which were cut with the desired size and stacked in a multilayer structure (each laminate is formed by 15 ceramic sheets). The green laminates were subject to a first de-binding treatment up to 1073 K in order to remove all their organic components and then sintered. Pressureless sintering was performed (Cristalox TS 150/250, TAV VACUUM FURNACES SPA, Caravaggio, Italy) under argon (99.99% purity, pressure maintained lower than 550

mbar) atmosphere at 2473 K for 30 minutes. Samples with different shapes and size were fabricated according to the various measurements requirements.

Two types of laminates were fabricated, one with a chemical composition of 100 vol% SiC and the other containing 80 vol% ZrB_2- 20 vol% SiC. The ZrB_2-SiC composites used for aerospace applications generally contain from 10 to 30 vol% SiC. The choice of adopting the composition 80 vol%ZrB_2-20 vol%SiC was made on the base of previous investigations of the properties of laminates containing different relative amount of the two components. The chosen composition represents one of the best compromise in terms of density and mechanical properties [20]. In addition, according to other works, this composition is one of the most used for hypersonic vehicles applications [21–23].

2.2   Characterization

The microstructure of specimens was investigated using SEM-EDS (SEM-FEG Assing SUPRA 25, Oberkochen, Germany, equipped with EDS Oxford analyzer); the crystallographic phases were identified using X-ray diffraction (Panalytical X'PERT PRO PW3040/60, Cu Kα radiation at 40 kV and 40 mA, Panalytical BV, Almelo, The Netherlands).

An emissivity measurement facility (EMF) working on Variable Black body source principle was used for the determination of laminates total emissivity; the equipment and the measurement method are described in more detail elsewhere [24,25]. The tests were performed on round samples with a diameter of 30 mm and thickness of 1.15 mm. A wavelength non-selective device was used for the total emissivity measurements. Total emissivity was tested on laminates with composition 100 vol% SiC and 80

6

vol%ZrB$_2$-20 vol%SiC; a set of three different specimens for each composition was tested in order to verify measurements repeatability

The emissivity was measured in the temperature range from 773 to 1830 K and the temperature was monitored using a GIRL IRM5 pyrometer (373 – 3273 K). The tests were performed under Argon inert atmosphere (purity of 99.998%) in order to minimize the oxidation process.

The laser flash technique was employed for the measurement of the most relevant thermophysical properties such as thermal diffusivity, specific heat and thermal conductivity. These properties were investigated using Flashline 4010, Anter Corporation (Pittsburgh, Pennsylvania, USA) equipment. Disks with diameter of 12.7 mm were obtained using diamond coated drills; both sides of the samples were polished with SiC waterproof sandpaper in order to obtain flat and parallel faces. The measurements were performed in argon atmosphere in order to minimize any oxidation process.

The thermal diffusivity (D) tests were performed from 450 to 1800 K with a heating rate of 5 K/min. The front side of disk-shaped samples was exposed to a laser pulse for a controlled very short time (0.3 ms pulse radiation); heat was absorbed and the consequent increase of temperature was measured on the bottom sample face. The Clark and Taylor method of analysis was used to calculate the thermal diffusivity of laminates. Laser flash technique was moreover used for the evaluation of the specific heat (C$_p$) from 450 to 1800 K; it was indirectly measured by comparison with a standard reference. Thermographite was selected as reference on the base of investigated temperature range: the energy required to heat the sample was compared with the amount of energy required to increase the temperature of the standard material. The

difference between the two experimental heat values was then used to determine the specific heat of the specimen. As laser flash cannot provide reliable values at low temperature, Differential Scanning Calorimetry (Perkin Elmer-1 DSC equipped with Intracooler 2P cooling accessory, Norwalk, Connecticut, USA) was used for measuring specific heat below 450K . The Pyris 8 software with Step-Scan program was used for the specific heat investigation: it involves a series of repeated heating and isothermal steps to cover the whole temperature range of interest (from 298 to 773 K). In this study heating steps of 20 K at a heating rate of 10 K/min between isothermal steps of 1 min were considered.

The thermal conductivity (κ) of SiC and composite multilayer was finally calculated employing Equation (1)

$$\kappa = \rho \cdot C_p \cdot D \qquad\qquad \text{Equation (1)}$$

where ρ is the density [kg/m^3], C_p the specific heat [J/kg·K] and D the thermal diffusivity [m^2/s].

The density (ρ) of laminates at room temperature was determined using Archimede's method. The variation of the specimens density as function of the temperature was calculated according to Equation (2) [26].

$$\rho(T) = \rho_{298K} \cdot \left[1 + \frac{\Delta l(T)}{l_{298K}}\right]^{-3} \qquad\qquad \text{Equation (2)}$$

Where ρ(T) is the density calculated at the desired temperature, Δl(T) is the experimentally measured linear thermal expansion and l_{298K} is the sample length at room temperature.

The thermal expansion behavior of laminates along X, Y and Z directions were measured using thermo-mechanical analysis (TMA - Setaram Instrumentation, France) from 298 to 1773 K with a heating rate of 10 K/min. For thermal expansion behavior test cuboid samples were prepared with a base size of 4×4 mm^2, while the thickness (around 8 mm) was used as testing direction. The argon atmosphere was maintained at a flow rate of 20 ml/min to ensure the equilibrium of temperature and prevent oxidation of samples. The coefficient of thermal expansion (CTE) of laminates in X, Y and Z directions was calculated from the thermal expansion curves.

3.   Results and discussion

3.1   Total emissivity

During atmospheric re-entry the space vehicles have to disperse in the surrounding atmosphere high heat fluxes present on their surface. The kinetic energy of a spacecraft in addition to its potential energy is indeed converted into heat fluxes before landing. Moreover due to the high gas rates and the thermal heat loads involved during re-entry, the molecules of oxygen and nitrogen passing through the bow shock become dissociated. Then the atoms can recombine again to form molecules in the gas phase or directly on the TPS surface. The energy coming from the exothermic recombination process results in an additional heat flux on the TPS surface or in the surrounding gas phase [25].

Thermal protection systems have to effectively manage these great heat fluxes; the emissivity, in addition to the catalytic efficiency and the surface roughness, plays an important role in the surface energy balance [27]. For a vehicle which operates under the high heat flux conditions typical of re-entry phase, a high emissivity value improves

the protection shield performance by reducing the temperature gradients and the thermal stresses within the component [28].

Fig. 1 shows the curves of total emissivity (ε) for the two materials under investigation as a function of temperature from 773 to 1830 K. Two different behaviors can be observed: silicon carbide shows only a small variation of ε value which seems not to be dependent on the temperature. The data for the composite laminates show a progressive increase of emissivity from 773 to 1273 K up to the maximum value of 0.88; for higher temperatures no significant change of emissivity was observed.

Hatzl et al. [30] performed emissivity measurements of sintered SiC in the temperature range from 773 K to 1273 K and reported a limited increase of total emissivity from values of approximately ε=0.81 at 773 K to ε=0.84 at 1273 K. These results are in agreement with those obtained using EMF equipment: in fact SiC laminates show only a small oscillation of emissivity values from 0.84 to 0.85. Similar values can moreover be observed at higher temperature: Schubler et al. [24] reported a roughly constant value of total emissivity of sintered SiC at about 0.855 in the temperature range from 1073 to 1753 K. Moreover Brandt et al. [31] show a very little increase of ε_{SiC} from 1273 to 1573 K (they are respectively ε=0.81 at 1273 K and ε=0.84 at 1573 K).

Emissivity higher than 0.8 is considered sufficient for the components which operate at both high and very high temperaturesTypical TPS design requires a high emissivity value so that most of the impinging convective heating is radiated out, resulting in a lower amount of heat being conducted into the underlying structure [32].

SiC samples were characterized before and after emissivity tests: X-ray diffraction measurements resulted in very similar spectra showing silicon carbide as the main

crystalline phase. Therefore the emissivity test did not involve the formation of any oxide layer on the specimens' surface or its thickness was too low to be detectable by XRD. These results are in agreement with the EDS analysis reported in Fig. 2b, which was performed on the area of sample surface shown in Fig. 2a.

The EDS analysis evidenced the presence of 64.8 at.% of carbon, 33.4 at.% of silicon and 1.8 at.% of oxygen; on the base of these semi-quantitative values we may suppose the formation of a small amount of SiO_2 which can be estimated to be under 1%.

In addition to SiC phase, it was also evident the presence of carbon mainly as contaminant coming from graphite flakes added as sintering aid for SiC and the carbonaceous residuals formed during the multilayer processing; The experimental data of emissivity for ZrB_2-SiC composite (Fig. 1) show an almost linear increment of total emissivity from 870 to 1100 K while at higher temperature ε values are rather constant, and slightly oscillate around an average value of 0.877.

The X-ray diffraction spectra of composite laminates before and after the emissivity tests were used to evaluate the modifications of the samples' surface.

The crystalline phases are reported and compared before and after the emissivity test in Fig. 3: the XRD spectrum of the as processed ZrB_2-SiC (Fig. 3a) shows the peaks corresponding to mainly ZrB_2 and SiC, which are the phases constituting the composite. The presence of carbon is due to surface contamination, as previously observed for 100 vol%SiC laminates. Comparing this spectrum to that collected for the composite after the emissivity tests (Fig. 3b), we can observe the presence of ZrO_2 and ZrC in addition to the peaks corresponding to ZrB_2 and SiC; the carbon peak was not observed.

11

Although the measurements have been performed in argon inert atmosphere it seems evident that an oxygen contamination took place that resulted in a limited oxidation. The process and the consequent formation of oxide is dependent on the partial pressure of oxygen. Depending on it, SiC can indeed be removed by active oxidation reaction or it can be oxidized forming SiO_2 which is then volatilized.

Both in the case of 100 vol% SiC and for composite containing 20 vol% SiC, no evidence of SiO_2 formation was found. Even though we could not experimentally evaluate the partial pressure of oxygen inside the test chamber, we can assume that it was too low to enable the formation of SiO_2.

The oxidation of ZrB_2 leads to the formation of ZrO_2 as the only stable condensed phase; the XRD spectrum of composite samples after emissivity tests (Fig. 3b) corroborates the presence of monoclinic zirconia. Under the considered experimental conditions the tetragonal system should be the most stable polymorph; nevertheless, in the literature are reported examples of monoclinic ZrO_2 obtained at temperature higher than the theoretical ones. For example, Rezaie et al. [33] investigated the behavior of ZrB_2-30vol%SiC composite exposed at 1773 K to a CO-CO_2 mixture with a low partial pressure of oxygen ($\sim 10^{-10}$ Pa): no silica protective layer was observed and on the samples surface an external porous layer consisting mainly of monoclinic ZrO_2 was formed.

The presence of low partial pressure of oxygen and a high temperature can promote the reaction between zirconia and the residual carbon resulting in the formation of ZrC according to the following reaction:

$$ZrO_2 + 3C \rightarrow ZrC + 2CO \qquad\qquad\qquad \text{Equation (3)}$$

By comparing the experimental emissivity values with those available in the literature, significant differences can be found although they are referred to the same temperature range. In addition, there is no agreement between the emissivity values measured by different authors. However, it should be taken into account that this property can be experimentally measured as a function of wavelength and by varying the direction of the emitted radiation, which allows to define total directional, normal or hemspherical emissivity. Moreover, emissivity values significantly depend on many factors such as oxidation, samples surface roughness, machining method, material composition and heat treatment [28,34]. The environmental conditions for the emissivity measurements can be quite different (from air pressure to high vacuum) and they can have a great influence on total emissivity; surface reactions can in fact occur and the formation of an oxide layer can change the surface properties.

All these reasons make difficult the comparison between the data reported in literature and the ones obtained in the present work. Wang et al. [35] reported the total emissivity of ZrB_2-20 vol%SiC composite with the addition of 2 vol% $MoSi_2$ as sintering aids; the total emissivity was not experimentally measured, but obtained from the spectral emissivity integrated over the infrared region. According to these results ε increases linearly from 0.63 to 0.92 in the temperature range from 1273 to 1873 K. These data result in underestimated values with respect to our experimental results, except that for highest temperature range.

Meng et al. [28] investigated the radiative properties of ZrB_2-20 vol%SiC-15 vol%C in the temperature range from 1273 to 2073 K. According to these authors, the total normal emissivity initially decreases from 0.91 to 0.72 in the temperature range 1273 −

1673 K, increases a little up to the value of 0.78 in the temperature range 1673 – 1873 K and for higher temperatures it rapidly decreases up to a value of 0.66.

3.2 Thermal expansion of laminates: coefficient of thermal expansion

Thermal expansion provides further information on thermomechanical behavior of SiC and composite laminates to be used in TPS structure design. The linear thermal expansion behavior of multilayer samples was investigated along the three spatial directions: the X direction is that parallel to tape casting one, Y is perpendicular both to the tape casting and the thickness directions and Z is along laminates' thickness. The variation of CTE was studied in the temperature range from 520 to 1773 K; the data at low temperature (from room temperature to 520 K) were obtained by fitting the experimental curve (Fig. 4).

As observed in previous investigations the thermal expansion curves of polycrystalline ceramics can be properly fitted by using a third order polynomial function; the trend of CTE curves for SiC is similar in the three spatial directions, so an average response curve has been obtained by least square fitting and reported as Equation (4). For ZrB_2-SiC a divergence of the curves at low temperature seems to exist; however for temperature higher than 700 K the differences are not significant. Equation (5) is obtained by fitting the experimental data in the whole temperature range. Both of the equations show $R^2 > 0.999$.

$$\left(\frac{\Delta l}{l_0}\right)_{SiC} (\times 10^{-6}) = 3.19 + 2.5 \cdot 10^{-3}T - 8.0 \cdot 10^{-7}T^2 + 6.0 \cdot 10^{-11}T^3 \qquad \text{Equation (4)}$$

$$\left(\frac{\Delta l}{l_0}\right)_{ZrB_2-20\%SiC} (\times 10^{-6}) = 3.97 + 4.4 \cdot 10^{-3}T - 2.0 \cdot 10^{-6}T^2 + 3.0 \cdot 10^{-10}T^3 \qquad \text{Equation (5)}$$

The thermal expansion coefficient of SiC is lower than that of the ZrB_2/SiC composite in the whole temperature range.

The CTE of ZrB_2 is higher than that of SiC, showing values of 6.98×10^{-6} K^{-1} for ZrB_2 and 5.48×10^{-6} K^{-1} for SiC in the temperature range from 298 to1793 K [36]. The addition of SiC slightly decreases the CTE of ZrB_2 as previously reported in literature [37].

As the thermal expansion coefficient of SiC laminates are comparable along the three spatial directions in the whole temperature range, this material can be considered isotropic from the thermal expansion point of view.

On the contrary, the composite showed differences in the CTE values for temperatures up to around 600 K according to this order: CTE(Y)>CTE(X)>CTE(Z). This difference is less evident along X and Y directions, which correspond to the casting plane. The thermal expansion along Z axis is lower for temperatures less than about 600 K, but it becomes very close to the values observed in the other directions at temperatures higher than 600 K.

The average value of CTEs in the temperature range from 520 to 1773 K was calculated to be 4.65×10^{-6} K^{-1} for SiC and 6.7×10^{-6} K^{-1} for 80 vol%ZrB_2-20 vol%SiC; the difference between the average experimental curves for the two materials is constant (around 1.8×10^{-6} K^{-1}) at temperatures higher than 700 K. This mismatch can cause the formation of stresses and the consequent development of cracks. There is a small number of works regarding the joint use of HTCs and UHTCs materials in a multifunctional component: our previous paper [39] shows preliminary results regarding the processing of hybrid laminates integrating ZrB_2-SiC composite layers in between

SiC ones. The integration of the two materials was successfully achieved, but the properties of the hybrid laminate should be improved. In fact the CTEs mismatch, in addition to the different shrinkage of the two materials occurring during the multilayer burnout and sintering, caused the development of micro-cracks. Hu et al. [40] successfully fabricated an integrated composite with a porous C_f/C-ZrB_2-SiC core in between two compact layers made of C_f/C-ZrB_2-SiC and C_f/C-SiC to be used as thermal protection system. Moreover Jimenez et al. [41] investigated the joining of SiC multilayers with ceramic matrix composite (C_f/SiC) using the MAX-Phase Ti_3SiC_2 as joining agent.

3.3 Specific Heat

The specific heat of laminates with composition 100 vol%SiC and 80 vol%ZrB_2-20 vol%SiC as a function of temperature is shown in Fig. 5.

The heat capacity of both materials under investigation increases with increasing the temperature; however, the specific heat of sintered SiC is higher than that of composite in the whole temperature range. The experimental data obtained by using DSC and laser flash methods in different temperature ranges are in good agreement with the values collected by Munro for a variety of α-SiC materials [42] and those reported in the NIST-JANAF tables for α-SiC [43]. A slight deviation from literature values can be observed at low temperatures: the value of 0.84 J/g K for SiC at 450 K could be underestimated because laser flash equipment shows a relatively high background noise at low temperature. This is due to the fact that the detector is in the lowest range of use; in fact, this effect progressively decreases at higher temperature. As a consequence, the laser flash results are affected by a higher error at low temperatures, while the experimental error decreases at higher ones.

The specific heat capacity of multilayer with composition ZrB_2-20vol%SiC was very similar to that reported by Patel et al. [44] for a material with the same relative volumetric amount of the two components, which was processed at 2273 K by hot pressing sintering.

3.4 Thermal diffusivity

Fig. 6 shows the temperature dependence of thermal diffusivity for SiC and ZrB_2-SiC composite in the temperature range from 475 to 1773 K.

The thermal diffusivity of both materials decreases with the increase of the temperature: this trend suggests that their conduction behavior is dominated by phonons, as it is the case for most of the polycrystalline materials [45]. The increase of temperature results in an enhancement of phonon scattering which has a drastic effect on thermal diffusivity. The value of D for the two materials under investigation was similar at the lowest experimental temperature (D~31.5 $\times 10^2$ cm^2/s at 475K). However, it should be noted that the experimental error is higher at low temperature and decreases with the temperature increase (in fact it is linked to an intrinsic low sensitivity of the instrument at low temperature).

Although the starting diffusivity values are comparable for the two kinds of laminates, the difference becomes significant at high temperature: for instance, at temperatures above 1373 K the thermal diffusivity of SiC is much smaller than that of ZrB_2-SiC composite (e.g. D~7.6 $\times 10^2$ cm^2/s for SiC and D~14.5 $\times 10^2$ cm^2/s for ZrB_2-SiC composite at 1775 K).

3.5 Thermal conductivity

17

The thermal conductivity was calculated as a function of temperature for SiC and the composite with chemical composition 80 vol%ZrB$_2$-20 vol%SiC by using Equation (1), which correlates the thermal diffusivity, the specific heat and the density. The bulk density of laminates is assumed to remain constant in the investigated temperature range.

The thermal conductivity of both materials under investigation (Fig. 7) shows a decreasing trend with the temperature increase; the thermal conductivity of SiC is lower than the composite one in the whole temperature range.

It is well known that the thermal conductivity of SiC depends on several factors: the grain size, the nature of grain boundaries and the presence of secondary phases [46].

According to Collins et al. [47] the grain size plays an important role in the heat conduction mechanism at temperatures lower than 300 K; at higher temperatures the phonon scattering dominates any other effects, so that the influence of grain size become less important.

A factor that has to be taken into account in our investigation is the presence of boron and carbon added as solid state sintering aids in the amount of 1 wt% and 3 wt% respectively. These quantities were calculated with respect to silicon carbide, which is the main component in SiC laminates, but the minor one (20 vol%) in composite laminates. The heat conduction can be significantly reduced by the presence of impurity atoms in the SiC lattice, which can increase the influence of phonon scattering. These impurities may come from the sintering aids added in order to enhance the densification process [48]. Sigl et al. [48] showed that thermal conductivities of B-doped SiC-based

materials was reduced to values of 100-150 W/mK, which are well below the 400 W/mK observed for single-crystal SiC.

Munro [42] investigated the thermal conductivity of α-SiC containing boron (0.4 wt%) and carbon (0.5 wt%) as sintering aids; a comparison of his results with those obtained in this work shows a good agreement of the observed trends (Fig. 7a). Nevertheless, the values of thermal conductivities of pressureless sintered multilayers of the current work are lower than those observed by Munro; this is probably due to a higher porosity of laminates with respect to that of the monolithic material sintered by Munro. Moreover the relative amount of boron added in the laminates under investigation was higher with respect to that adopted by Munro, and this confirms the detrimental effect of this sintering aid on the thermal conductivity of SiC.

The thermal conductivity of ZrB_2-SiC composites is expected to be similar to that of pure ZrB_2 (85 W/mK at room temperature).

The literature data about the thermal conductivity of polycrystalline ZrB_2-based material are widely scattered (see Fig. 7b), very likely because this property is influenced by several factors such as the investigation method, the presence and the amount of sintering additives and impurities, the grain sizes and the porosity. This dispersion of data is more important at temperatures below 750 K, where the κ values were reported to be in the range from 45 to 135 W/mK, but conductivity values in the more narrow range between 60 and 80 W/mK were measured at temperatures higher than 1250 K [50–53].

For diboride-based ceramics conductivity results from both electron and phonon contributions, thanks to the metallic and covalent nature of their bonding.

Our experimental results presented in Fig. 7b show a decrease of composite's thermal conductivity with the increase of temperature. According to all the curves depicted in Fig. 7b the thermal conductivity seems to move towards a constant value at temperature higher than 1100 K. This trend was previously observed and justified by Grimvall [54] considering the fact that the heat capacity, the phonons velocity and their mean free path become constant at high temperature. This plateau was so interpreted as the saturation limit of phonon-controlled thermal conductivity.

For TPS applications a high value of thermal conductivity is desirable because it can enhance the thermal shock resistance by the limiting thermal gradient and stresses within the material.

4. Conclusions

The aim of the present study was to investigate the most important thermal properties influencing the behavior of materials at high temperature and under the severe environmental conditions involved during space missions.

The total emissivity of laminates containing 100 vol%SiC and composites with composition 80 vol%ZrB_2– 20 vol%SiC were investigated and compared. The total emissivity of SiC laminates (around 0.85) only slightly changed in the whole temperature range. The trend observed for the ZrB_2-SiC composite was quite different, showing an increment of emissivity as a function of temperature up to a maximum value of 0.88, which was reached and maintained for temperatures above 1273 K. Both materials showed high values of total emissivity which are required for TPS applications.

The investigation of the thermal properties of SiC and composite laminates involved the measurement and comparison of their thermal expansion coefficient, specific heat, thermal diffusivity and conductivity. The CTE of both materials increases as the temperature increases, but the CTE of SiC is constantly lower with respect to the composite one. This thermal mismatch can cause the development of stresses when these materials are joined together; however the CTE of ZrB_2-SiC composites can be decreased by increasing the SiC content.

The thermal diffusivity and conductivity of SiC and ZrB_2-SiC multilayers show a decreasing trend with the increase of the temperature, but for both properties the values for SiC are well below those for the composite. Therefore the higher thermal conductivity of ZrB_2-SiC laminates combined with the high emissivity at high temperatures and the high melting point represent desirable properties for extreme environment applications. However, SiC can grant lightness and passivation behavior in oxidative environments. Hybrid structures integrating both of these materials could be designed, thus exploiting all their attractive properties for applications as TPS for space vehicles. For this purpose, concerns related to the CTE mismatch and the different shrinkage during material process need to be addressed. Differences in term of CTE could be reduced by reconsidering the ZrB_2:SiC ratio in the composite. On the other hand the different sintering shrinkage occurring for SiC and composite layers causes the formation of residual stresses and could lead to the failure of the laminates. An homogenization of powders grain size, thus reducing the grain size of ZrB_2 starting powder, could reduce the residual stresses and promote the integration of the two materials.

Acknowledgements

References

[1]   L. Chauvin, R. Erb, D. Greenshields, J.E. Pavlosky, C.L. Statham, Apollo thermal-protection system development, J. Spacecr. Rockets. 7 (1970) 727–734. doi:10.2514/3.30027.

[2]   D. Olynick, Y.K. Ghent, M.E. Tauber, Forebody TPS Sizing with Radiation and Ablation for the Stardust Sample Return Capsule, AIAA Thermophys. Conf. 32 (1997) 18. doi:10.2514/6.1997-2474.

[3]   P.A. Cooper, P.F. Holloway, The Shuttle Tile Story, Astronaut. Aeronaut. (1981) 24–36.

[4]   D. Glass, Ceramic Matrix Composite (CMC) Thermal Protection Systems (TPS) and Hot Structures for Hypersonic Vehicles, in: 15th AIAA Int. Sp. Planes Hypersonic Syst. Technol. Conf., 2008. doi:10.2514/6.2008-2682.

[5]   D.C. Freeman Jr., T.A. Talay, R.E. Austin, Reusable launch vehicle technology program, Acta Astronaut. 41 (1997) 777–790.

[6]   R.I. Baumgartner, Venturestar^{TM} single stage to orbit reusable launch vehicle program overview, in: AIP Conf. Proc., 1997: pp. 1033–1040.

[7]   and K.E.W. M. L. Blosser, C. C. Poteet, R. R. Chen, J. T. Dorsey, I. H. Schmidt, R. K. Bird, Development of Advanced Metallic, Thermal-Protection-System Prototype Hardware, J. Spacecr. Rockets. 41 (2004) 183–194.

[8]   and S.-Y.H. Carl C. Poteet, Hasan Abu-Khajeel, Preliminary Thermal-Mechanical Sizing of a Metallic Thermal Protection System, J. Spacecr. Rockets. 41 (2004) 173–182.

[9]   R. Savino, M. De Stefano Fumo, D. Paterna, A. Di Maso, F. Monteverde, Arc-jet testing of ultra-high-temperature-ceramics, Aerosp. Sci. Technol. 14 (2010) 178–187. doi:10.1016/j.ast.2009.12.004.

[10]   X. Jin, R. He, X. Zhang, P. Hu, Ablation behavior of ZrB2-SiC sharp leading edges, J. Alloys Compd. 566 (2013) 125–130. doi:10.1016/j.jallcom.2013.03.067.

[11]   S.-Q. Guo, Densification of ZrB2-based composites and their mechanical and physical properties: A review, J. Eur. Ceram. Soc. 29 (2009) 995–1011. doi:10.1016/j.jeurceramsoc.2008.11.008.

[12]   M. Pavese, P. Fino, A. Ortona, C. Badini, Potential of SiC multilayer ceramics for high temperature applications in oxidising environment, Ceram. Int. 34 (2008) 197–203. doi:10.1016/j.ceramint.2006.09.008.

[13]   M.M. Opeka, I.G. Talmy, J.A. Zaykoski, Oxidation-based materials selection for 2000°C + hypersonic aerosurfaces: Theoretical considerations and historical experience, in: J. Mater. Sci., 2004: pp. 5887–5904. doi:10.1023/B:JMSC.0000041686.21788.77.

[14]   S.R. Levine, E.J. Opila, M.C. Halbig, J.D. Kiser, M. Singh, J.A. Salem, Evaluation of ultra-high temperature ceramics foraeropropulsion use, J. Eur. Ceram. Soc. 22 (2002) 2757–2767. doi:10.1016/S0955-2219(02)00140-1.

[15]   H.G. WC Tripp, HH Davis, Effect of an SiC addition on the oxidation of ZrB2, Ceram. Bull. 52 (1973) 612–616.

[16]   S. Biamino, V. Liedtke, C. Badini, G. Euchberger, I. Huertas Olivares, M. Pavese, P. Fino, Multilayer SiC for thermal protection system of space vehicles: Manufacturing and testing under simulated re-entry conditions, J. Eur. Ceram. Soc. 28 (2008) 2791–2800. doi:10.1016/j.jeurceramsoc.2008.04.006.

[17]   B. Schneider, A. Guette, R. Naslain, M. Cataldi, A. Costecalde, A theoretical and experimental approach to the active-to-passive transition in the oxidation of silicon carbide - Experiments at high temperatures and low total pressures, J. Mater. Sci. 33 (1998) 535–547. doi:10.1023/A:1004313022769.

[18]   N.S. Jacobson, D.L. Myers, Active oxidation of SiC, Oxid. Met. 75 (2011) 1–25. doi:10.1007/s11085-010-9216-4.

[19]   D. J. Barcena, M. Lagos, I. Agote, C. Jimenez, X. Hernandez, C. Badini, E. Padovano, S. Gianella, and C.W. Gaia, V. Liedtke, K. Mergia, S. Messoloras, P. Yialouris, Y. Panayiotatos, A. Ortona, C. D'Angelo, SMARTEES FP7 Space Project – Towards a New TPS Reusable Concept for Atmospheric Reentry from Low Earth Orbit, in: Proc. 7th Eur. Work. TPS Hot Struct., 2013: pp. 8–10.

[20]   E. Padovano, C. Badini, S. Biamino, M. Pavese, W.S. Yang, P. Fino, Pressureless sintering of ZrB2-SiC composite laminates using boron and carbon as sintering aids, Adv. Appl. Ceram. 112 (2013) 478–486. doi:10.1179/1743676113Y.0000000119.

[21]   A.J. J.F.Justin, Ultra High Temperature Ceramics : Densification , Properties and Thermal Stability, (2011) 1–11.

[22]   F. Monteverde, A. Bellosi, Oxidation of ZrB2-Based Ceramics in Dry Air, J. Electrochem. Soc. 150 (2003) B552. doi:10.1149/1.1618226.

[23]   A.L. Chamberlain, W.G. Fahrenholtz, G.E. Hilmas, D.T. Ellerby, High-strength zirconium diboride-based ceramics, J. Am. Ceram. Soc. 87 (2004) 1170–1172. doi:10.1111/j.1551-2916.2004.01170.x.

[24]   G.H. and S.P. M. Schubler, M. Auweter-Kurtz, Characterization of candidate materials for the catalytic re-entry experiment philux on expert., in: Therm. Prot. Syst. Hot Struct. - Proceeding 5th Eur. Work. TPS Hot Struct., 2006.

[25]   M. Schüßler, M. Auweter-Kurtz, G. Herdrich, S. Lein, Surface characterization of metallic and ceramic TPS-materials for reusable space vehicles, Acta Astronaut. 65 (2009) 676–686. doi:10.1016/j.actaastro.2009.01.048.

[26]   J.W. Zimmermann, G.E. Hilmas, W.G. Fahrenholtz, R.B. Dinwiddie, W.D. Porter, H. Wang, Thermophysical properties of ZrB2 and ZrB2-SiC ceramics, J. Am. Ceram. Soc. 91 (2008) 1405–1411. doi:10.1111/j.1551-2916.2008.02268.x.

[27]   T.H. Squire, J. Marschall, Material property requirements for analysis and design of UHTC components in hypersonic applications, J. Eur. Ceram. Soc. 30 (2010) 2239–2251. doi:10.1016/j.jeurceramsoc.2010.01.026.

[28]   S. Meng, H. Chen, J. Hu, Z. Wang, Radiative properties characterization of ZrB2-SiC-based ultrahigh temperature ceramic at high temperature, Mater. Des. 32 (2011) 377–381. doi:10.1016/j.matdes.2010.06.007.

[30]   S. Hatzl, M. Kirschner, V. Lippig, T. Sander, C. Mundt, M. Pfitzner, Direct measurements of infrared normal spectral emissivity of solid materials for high-temperature applications, Int. J. Thermophys. 34 (2013) 2089–2101. doi:10.1007/s10765-013-1531-y.

[31]   R. Brandt, G. Neuer, P. Pohlmann, E. Schreiber, Thermisches Verhalten von C / C-SiC, (1998) 1–25.

[32]   J.F. Justin, A. Jankowiak, Ultra High Temperature Ceramics: Densification, Properties and Thermal Stability, AerospaceLab J. 3 (2011) AL3-08.

[33]   A. Rezaie, W.G. Fanrenholtz, G.E. Hilmas, Oxidation of zirconium diboride-silicon carbide at 1500°C at a low partial pressure of oxygen, J. Am. Ceram. Soc. 89 (2006) 3240–3245. doi:10.1111/j.1551-2916.2006.01229.x.

[34]   T.K. V.Musilova, P. Hanzelka, Emissivity and in situ measurement of amount of water condensed on metallic sample, in: Proc. 11th Cryog. 2010 IIR Int. Conf., 2010: pp. 37–42.

[35]   F. Wang, L. Cheng, Y. Xie, J. Jian, L. Zhang, Effects of SiC shape and oxidation on the infrared emissivity properties of ZrB2-SiC ceramics, J. Alloys Compd. 625 (2015) 1–7. doi:10.1016/j.jallcom.2014.09.191.

[36]   J. Shackelford, S.H.K. Y-H Han, S. Kim, Materials Science and Engineering Handbook, Third Edit, 2001. doi:10.1126/science.232.4757.1485.

[37]   A. Paul, J. Binner, B. Vaidhyanathan, UHTC Composites for Hypersonic Applications, in: Ultra-High Temp. Ceram. Mater. Extrem. Environ. Appl., 2014: pp. 144–166. doi:10.1002/9781118700853.ch7.

[39]   E. Padovano, C. Badini, E. Celasco, S. Biamino, M. Pavese, P. Fino, Oxidation behavior of ZrB2/SiC laminates: Effect of composition on microstructure and mechanical strength, J. Eur. Ceram. Soc. 35 (2015) 1699–1714. doi:10.1016/j.jeurceramsoc.2014.12.029.

[40]   C. Hu, S. Pang, S. Tang, Y. Wang, H.M. Cheng, An integrated composite with a porous Cf/C-ZrB2-SiC core between two compact outer layers of Cf/C-ZrB2-SiC and Cf/C-SiC, J. Eur. Ceram. Soc. 35 (2015) 1113–1117. doi:10.1016/j.jeurceramsoc.2014.10.005.

[41]   C. Jiménez, K. Mergia, M. Lagos, P. Yialouris, I. Agote, V. Liedtke, S. Messoloras, Y. Panayiotatos, E. Padovano, C. Badini, C. Wilhelmi, J. Barcena, Joining of ceramic matrix composites to high temperature ceramics for thermal protection systems, J. Eur. Ceram. Soc. 36 (2016) 443–449. doi:10.1016/j.jeurceramsoc.2015.09.038.

[42]   R.G. Munro, Material Properties of a Sintered α-SiC, J. Phys. Chem. Ref. Data. 26 (1997) 1195–1201. doi:10.1063/1.556000.

[43]   M. Chase Jr., Tables, NIST-JANAF Thermochemical, J. Phys. Chem. Ref. Data. (1998) 1952. doi:10.1021/ac991732g.

[44]   M. Patel, V.V.B. Prasad, V. Jayaram, Heat conduction mechanisms in hot pressed ZrB2 and ZrB2-SiC composites, J. Eur. Ceram. Soc. 33 (2013) 1615–1624. doi:10.1016/j.jeurceramsoc.2013.03.006.

[45]   D.M. Liu, B.W. Lin, Thermal conductivity in hot-pressed silicon carbide, Ceram. Int. 22 (1996)

407–414. doi:10.1016/0272-8842(95)00125-5.

[46] L.L. Snead, T. Nozawa, Y. Katoh, T.S. Byun, S. Kondo, D.A. Petti, Handbook of SiC properties for fuel performance modeling, J. Nucl. Mater. 371 (2007) 329–377. doi:10.1016/j.jnucmat.2007.05.016.

[47] A.K. Collins, M.A. Pickering, R.L. Taylor, Grain size dependence of the thermal conductivity of polycrystalline chemical vapor deposited β-SiC at low temperatures, J. Appl. Phys. 68 (1990) 6510–6512. doi:10.1063/1.346852.

[48] L.S. Sigl, Thermal conductivity of liquid phase sintered silicon carbide, J. Eur. Ceram. Soc. 23 (2003) 1115–1122. doi:10.1016/S0955-2219(02)00271-6.

[50] E.V. Tye, R.P. ; Clougherty, Thermal and electrical conductivities of some electrically conducting compounds, in: Proc. Fifth Symp. Thermophys. Prop., 1970.

[51] M.J. Thompson, W.G. Fahrenholtz, G.E. Hilmas, Elevated Temperature Thermal Properties of ZrB2 with Carbon Additions, J. Am. Ceram. Soc. (2012) n/a-n/a. doi:10.1111/j.1551-2916.2011.05034.x.

[52] L. Zhang, D.A. Pejaković, J. Marschall, M. Gasch, Thermal and Electrical Transport Properties of Spark Plasma-Sintered HfB2 and ZrB2 Ceramics, J. Am. Ceram. Soc. 94 (2011) 2562–2570. doi:10.1111/j.1551-2916.2011.04411.x.

[53] J. Lonergan, Thermophysical properties of reaction processed zirconium diboride, Dr. Diss. (2014). http://scholarsmine.mst.edu/doctoral_dissertations/2348.

[54] G. Grimvall, Thermal conductivity, Thermophys. Prop. Mater. (1999) 255–285. doi:http://dx.doi.org/10.1016/B978-044482794-4/50017-6.

Fig. 1: Comparison of total emissivity of multilayer with composition 100 vol% SiC and 80 vol%ZrB$_2$-20vol%SiC.

Fig. 2: (a) SEM micrograph of SiC sample surface; (b)EDS analysis carried out on SiC sample.

Fig. 3: XRD spectra of 80vol%ZrB$_2$-20vol%SiC before (a) and after (b) emissivity test.

Fig. 4: Thermal expansion coefficient of (a) SiC and (b) ZrB$_2$-SiC multilayer as function of temperature along X, Y and Z directions.

Fig. 5: Specific heat of ceramic under investigation: (a) SiC; (b) ZrB$_2$ and ZrB$_2$-20%SiC composite

Fig. 6: Thermal diffusivity of SiC and ZrB$_2$-SiC multilayer as a function of temperature.

Fig. 7: Thermal conductivity as a function of temperature for (a) SiC and (b) ZrB$_2$-SiC laminates.
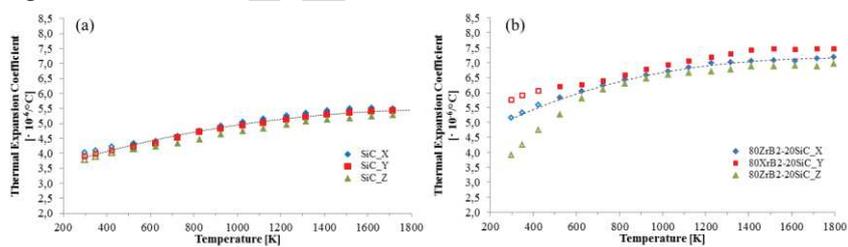

Fig. 1

26

Fig. 2

Fig. 3

Fig. 4

Fig. 5

Fig. 6

Fig. 7